# Melanin and blood concentration in human skin studied by multiple regression analysis: experiments

**M Shimada[1], Y Yamada[2,3], M Itoh[4] and T Yatagai[4]**

[1] Department of Integrated Neuroscience, Tokyo Institute of Psychiatry, Kamikitazawa 2-1-8, Setagaya, Tokyo, 156-8585, Japan
[2] Department of Mechanical Engineering and Intelligent Systems, University of Electro-Communications, Chofugaoka 1-5-1, Chofu, Tokyo, 182-8585, Japan
[3] Institute of Human Science and Biomedical Engineering, National Institute of Advanced Industrial Science and Technology, Namiki 1-2-1, Tsukuba, Ibaraki, 305-8564, Japan
[4] Institute of Applied Physics, University of Tsukuba, Ten-noh-dai 1-1-1, Tsukuba, Ibaraki, 305-8573, Japan

E-mail: shimada@prit.go.jp

**Abstract**
Knowledge of the mechanism of human skin colour and measurement of melanin and blood concentration in human skin are needed in the medical and cosmetic fields. The absorbance spectrum from reflectance at the visible wavelength of human skin increases under several conditions such as a sunburn or scalding. The change of the absorbance spectrum from reflectance including the scattering effect does not correspond to the molar absorption spectrum of melanin and blood. The modified Beer–Lambert law is applied to the change in the absorbance spectrum from reflectance of human skin as the change in melanin and blood is assumed to be small. The concentration of melanin and blood was estimated from the absorbance spectrum reflectance of human skin using multiple regression analysis. Estimated concentrations were compared with the measured one in a phantom experiment and this method was applied to *in vivo* skin.

## 1. Introduction

Measurement of melanin and blood concentration in human skin is needed in the medical and cosmetic fields because human skin colour mainly depends on the colours of melanin and blood (Feather *et al* 1988). To measure them from the reflectance spectrum of human skin, it is necessary to analyse light propagation in human skin at the visible wavelength range. This analysis, however, has not been established because the multi-layered structure and strong forward scattering of human skin complicates light propagation.

The methods of analysing the reflectance spectrum of human skin are put into two categories. One of them is calculation of light propagation at each wavelength. For a strong forward scattering medium such as biological tissue, it is possible to approximately solve the reflectance by the Monte Carlo method (Wang and Jacques 1992, Wang *et al* 1995). Though the Monte Carlo method has come to be used for the analysis of skin colour as computers have been developed (Kienle *et al* 1995, Verkruysse *et al* 1999, Barton *et al* 1998, Lu *et al* 2000), this method needs a lot of calculation time. The Kubelka–Munk theory describing light propagation in only two directions had previously been used widely for the colour analysis of the scattering medium (Hasegawa *et al* 1981, Anderson *et al* 1980, Anderson and Parrish 1981, van Gemert *et al* 1989, Wan *et al* 1981). These methods require the optical coefficient and geometrical information of each layer and neglect information of the shape of the reflectance spectrum of human skin.

Another category is statistical spectrum analysis. It is useful for a limited object such as reflectance spectra of skin. Principal component analysis (Imai *et al* 1996, Tsumura *et al* 1999a) and independent component analysis (Tsumura *et al* 1999b) are applied to image processing and measurement of melanin and blood concentration. These methods use only reflectance spectra and it is difficult to incorporate the optical and geometrical information of human skin.

We proposed multiple regression analysis (Johnson and Bhattacharyya 1996) based on the modified Beer–Lambert law (Nomura *et al* 1997, 1989, Hiraoka *et al* 1993, Delpy *et al* 1988, Matcher 1993) as the spectrum analysis of human skin (Shimada *et al* 2000). This method incorporates multiple regression analysis as spectrum analysis, and the modified Beer–Lambert law as a light propagation model. It is possible to measure melanin and blood concentration by this method in a shorter calculation time.

## 2. Theoretical formulation

### 2.1. The modified Beer–Lambert law with average geometrical path lengths in scattering media

An absorbance spectrum $A(\lambda)$ at each wavelength $\lambda$ is defined from the reflectance spectrum $R(\lambda)$ of the skin of the face or arm which is considered to be a semi-infinite medium

$$A(\lambda) = -\log_{10} R(\lambda). \tag{1}$$

$A(\lambda)$ of the homogeneous medium is shown as the modified Beer–Lambert law

$$A(\lambda) = \varepsilon(\lambda)C\bar{l}(\lambda, C) + G(\lambda) \tag{2}$$

where $\varepsilon(\lambda)$ is a molar absorption coefficient (Anderson *et al* 1980, Anderson and Parrish 1981), $C$ is the molar concentration, $\bar{l}(\lambda)$ is the mean path length and $G(\lambda)$ is scattering loss. $A(\lambda)$ of a multi-layered medium whose scattering and molar absorption coefficient are different from each layer is expressed as the sum of absorbance of each layer $A_i(\lambda)$ ($i = 1, \ldots, m$), as shown in figure 1.

$$A(\lambda, C_1, \ldots, C_m) = \sum_{i=1}^{m} A_i(\lambda, C_i) + G(\lambda) = \sum_{i=1}^{m} \varepsilon_i(\lambda)C_i(\lambda)\bar{l}_i(\lambda, C_i) + G(\lambda). \tag{3}$$

The subscript $i$ denotes the $i$th layer. $\bar{l}_i(\lambda, C_i)$ is the mean path length of the $i$th layer. $\bar{l}_i(\lambda, C_i)$ and $G(\lambda)$ depend on the wavelength, because the scattering coefficient is different at each wavelength. For reflectance of semi-infinite media measured by the integrating sphere, as the scattering strengthens, $\bar{l}_i(\lambda)$ becomes short and $G(\lambda)$ becomes large. $\bar{l}_i(\lambda)$ becomes
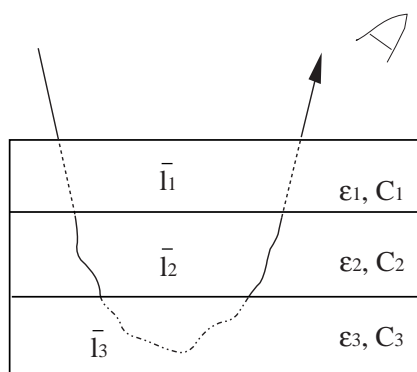
**Figure 1.** Schematic of mean path length of $i$th layer $\bar{l}_i$.

short as $C_i$ increases while $G(\lambda)$ is independent of $C_i$. The change of $\bar{l}_i(\lambda)$ is large as scattering strengthens.

It is possible to approximate $\bar{l}_i(\lambda) \simeq \bar{l}_i(\lambda, C_i)$ if $C_i$ varies in a small range. $\Delta A_i(\lambda)$ is defined as a change in the absorbance spectrum caused by a change of concentration of the $i$th chromophore $\Delta C_i$:

$$\Delta A_i(\lambda) = \varepsilon_i(\lambda)\Delta C_i \bar{l}_i(\lambda). \tag{4}$$

This equation shows $\Delta A_i(\lambda)$ is proportional to $\Delta C_i$. The shape of $\Delta A_i(\lambda)$ including $\bar{l}_i(\lambda)$, that is to say, the effect of scattering, is of a different shape from that of $\varepsilon_i(\lambda)$.

### 2.2. Multiple linear regression analysis

A relationship between two variable sets $x_{ij}$ and $y_j$ $(i = 1, 2, \ldots, p)$ $(j = 1, 2, \ldots, q)$ is expressed as a linear equation

$$y_j = \sum_{i=1}^{p} \beta_i x_{ij} + e_j. \tag{5}$$

$x_{ij}$ and $y_j$ are named as a predictor variable and a response variable, respectively. $p$ is the number of the predictor variable and $q$ is the number of the set including the $p$ predictor variables and the response variable. $e_j$ is unknown error components that cannot be explained by $x_{ij}$. The multiple regression analysis is to estimate unknown parameter $\beta_i$ from equation (5) using the least squares fitting. $\hat{y}_i$ and $\hat{\beta}_i$ denoting $y_i$ and $\beta_i$ estimated by the regression analysis, respectively, are expressed as

$$\hat{y}_j = \sum_{i=1}^{p} \hat{\beta}_i x_{ij}. \tag{6}$$

The strength of the linear relation $R^2$ is defined as the square of the coefficient of correlation $R$

$$R^2 = \left[ \frac{\sum_j (y_j - \bar{y}_j)(\hat{y}_j - \bar{\hat{y}}_j)}{\sqrt{\sum_j (\hat{y}_j - \bar{\hat{y}}_j)^2}\sqrt{\sum_j (y_j - \bar{y}_j)^2}} \right]^2 \tag{7}$$

where $\bar{y}_j$ and $\bar{\hat{y}}_j$ show the average of $y$ and $\hat{y}$, respectively, and these values correspond. $R^2$ is from 0 to 1 and the approximation is good as $R^2$ is nearer to 1.

## 2.3. Application of the modified Beer–Lambert law to human skin

Human skin is divided into three layers, epidermis, dermis and subcutaneous fat from the surface (Anderson *et al* 1980, Anderson and Parrish 1981, van Gemert *et al* 1989). Melanin and blood in vessels, two main chromophores in human skin, are in the epidermis and the dermis, respectively. To simplify, the subcutaneous fat including no remarkable chromophores is assumed to completely diffuse and reflect light at the whole visible wavelength. The change in scattering properties is neglected because the scattering properties of the chromophores are not as the strong as the dermis.

The change in $C_m$ and $C_b$ in human skin is assumed to be so small that $\bar{l}(\lambda)$ is independent of the concentrations of the chromophore $C$. The subscripts 'm' and 'b' denote melanin and blood. The absorbance spectrum of skin $A_{skin}(\lambda)$ is expressed as

$$A_{skin}(\lambda) = \varepsilon_m(\lambda)C_m\bar{l}_m(\lambda) + \varepsilon_b C_b \bar{l}_b(\lambda) + A_0(\lambda) \tag{8}$$

$$A_0(\lambda) = A_0'(\lambda) + G(\lambda) \tag{9}$$

where $A_0'(\lambda)$ is a spectrum of all chromophores in human skin except melanin and blood. Equation (8) is translated to (10) using equation (4):

$$A_{skin}(\lambda) = \frac{C_m}{\Delta C_m}\Delta A_m(\lambda) + \frac{C_b}{\Delta C_b}\Delta A_b(\lambda) + A_0(\lambda) \tag{10}$$

$$\Delta A_m(\lambda) = \varepsilon_m(\lambda)\Delta C_m\bar{l}_m(\lambda) \qquad \Delta A_b(\lambda) = \varepsilon_b(\lambda)\Delta C_b\bar{l}_b(\lambda). \tag{11}$$

$\bar{l}_i$ ($i = $ m, b) of equation (11) and that of equation (8) must correspond. If $\Delta A_m(\lambda)$, $\Delta A_b(\lambda)$ and $A_0(\lambda)$ are known, it is possible to estimate $C_m/\Delta C_m$ and $C_b/\Delta C_b$ of arbitrary $A_{skin}(\lambda)$ using multiple regression analysis.

## 3. Experiments

### 3.1. Fabrication of skin phantoms and measurement of their reflectance spectra

To simplify, the human skin was assumed to consist of three layers: epidermis including melanin, dermis including blood and subcutaneous fat. A gelatin solution was prepared by mixing gelatin powder (Miyagi Chemical Industrial Co. Ltd., Japan) with distilled water at a weight ratio of 33.3%. Scattering matter of epidermis phantoms was fabricated by adding intralipid (PharmaciaAB, Sweden) to the gelatin solution of 5% weight ratio. Squid ink whose principal component is melanin was used instead of pure melanin because pure melanin is unavailable. We name the squid ink solution as melanin in this paper. The melanin solutions of 0.0, 0.025, 0.050, 0.075, 0.100 g were injected in the scattering matter of epidermis (10.0 g) and mixed to make the homogeneous phantoms. Temperature of the scattering matter was kept at about 40 degrees during the making of the phantoms to avoid change in the scattering coefficient. If it is too hot, water in the scattering matter evaporates. If it is too cold, the scattering matter hardens. The scattering matters with different melanin concentrations (6.0 g) were hardened in dishes with a diameter of 60 mm to fabricate the five kinds of epidermis phantoms with thickness of 2.5 mm. The scattering matter of the dermis phantom was fabricated by adding intralipid to the gelatin solution of 13.3% weight ratio. After the blood was heparinized and shaken in the air to oxygenate, the blood (0.0, 0.025, 0.050, 0.075 and 0.100 g concentration) was mixed with the scattering matter of the dermis (20.0 g). The scattering matter with different blood concentrations of 15.0 g was hardened in the same manner to fabricate the five dermis phantoms with a thickness of 6.3 mm. A subcutaneous fat phantom was made by spreading BaSO$_4$ of about 4.0 g on the bottom of a dish. We overlaid the subcutaneous fat phantom with a dermis phantom
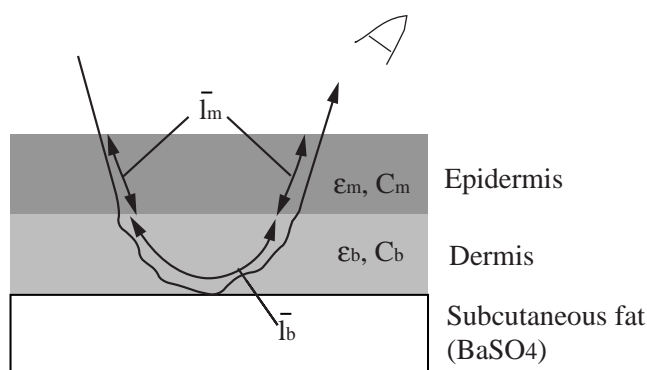
**Figure 2.** Schematic of skin phantom composed by epidermis, dermis and subcutaneous fat from surface.

and an epidermis phantom as shown in figure 2 and made 25 kinds of three-layered skin phantoms. All reflectance spectra of skin phantoms were measured by the UV-3100 UV-VIS-NIR spectrophotometer (Shimadzu, Japan) at the whole wavelength from 400 to 700 nm with a 10 nm pitch. The ISR-3100 integrating sphere (Shimadzu, Japan) with a 60 mm of diameter is corporated into the spectrophotometer for measurement reflectance spectra. The input and detected area for reflectance measurement were $7 \times 9$ mm and 18 mm in diameter, respectively. The absorbance spectra of the chromophores were obtained from transmittance spectra $-\log_{10} T(\lambda)$.

Melanin and blood were dissolved in saline with the weight ratio 0.5 and 1%, respectively. We measured the transmittance spectra of the chromophore solution in the cell with thickness of 10 mm by the UV-3100 UV-VIS-NIR spectrophotometer at the whole wavelength from 400 to 700 nm with a 10 nm pitch. The absorbance spectra of skin phantoms were obtained from reflectance spectra $-\log_{10} R(\lambda)$.

### 3.2. In vivo measurement of reflectance spectra of the skin exposed to UV light and hot water

A reflectance spectrum of human skin changes through exposure to UV light or hot water because of an increase in melanin and blood. Reflectance spectra of three persons' arms were measured before and 2, 9 and 16 days after exposure to UV light of 2MED at the same position. 1MED is the minimum erythermal dose and is defined as UV energy received for a precise period of time. Reflectance spectra of five other persons' arms were measured before and 2, 6, 31 and 61 min after bathing in water at $47^\circ$C for 3 min. All reflectance spectra of human skin were measured by the CM-1000HR colorimeter (Minolta Co., Japan) with the integrating sphere at the whole wavelength from 400 to 700 nm with a 10 nm pitch.

## 4. Results and discussion

### 4.1. Estimation of melanin and blood concentrations in the skin phantoms

The five epidermis phantoms are named $E(i)$ phantom ($i = 0, 1, 2, 3, 4$) in which $i$ means the five kinds of concentration of melanin. In the same manner, the five dermis phantoms named $D(j)$ phantom ($j = 0, 1, 2, 3, 4$) in which $j$ means the five kinds of concentration of blood. The three-layered skin phantoms which consist of $E(i)$ phantom, $D(j)$ phantom and subcutaneous fat phantom are named $E(i)D(j)$ phantom. $A_{E(i)D(j)}(\lambda)$ is the absorbance
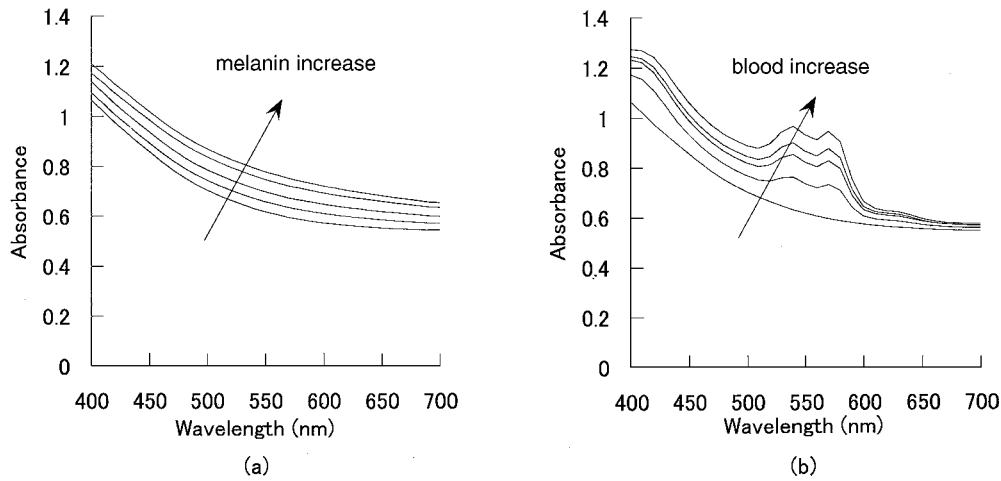
**Figure 3.** Absorbance spectra of three-layered skin phantoms (a) $A_{E(i)D(0)}(\lambda)$ $(i = 0, 1, 2, 3, 4)$. Absorbance spectra decrease as melanin concentration in epidermis phantom increases. (b) $A_{E(0)D(j)}(\lambda)$ $(j = 0, 1, 2, 3, 4)$. Absorbance spectra decrease as the blood concentration in the epidermis phantom increases.

spectrum of $E(i)D(j)$ phantom. $A_{E(i)D(0)}(\lambda)$ $(i = 0, 1, 2, 3, 4)$ shown in figure 3(a) decrease as $i$ increases. $A_{E(0)D(j)}(\lambda)$ $(j = 0, 1, 2, 3, 4)$ shown in figure 3(b) decrease as $j$ increases. No change in the shape of the spectrum appears in figure 3(a) and (b).

If $\Delta A_\mathrm{m}(\lambda)$ in equation (10) is defined as the average of change in the absorbance spectrum when $i$ increases by only one, $\Delta A_\mathrm{m}(\lambda)$ follows as

$$\Delta A_\mathrm{m}(\lambda) = \frac{\sum_{i=0}^{3} \left| A_{E(i+1)D(0)}(\lambda) - A_{E(i)D(0)}(\lambda) \right|}{4} = \frac{A_{E(4)D(0)}(\lambda) - A_{E(0)D(0)}(\lambda)}{4}. \quad (12)$$

$\Delta A_\mathrm{m}(\lambda)$ only contained information of $A_{E(i)D(0)}(\lambda)$ $(i = 0, 4)$. So, we defined $\Delta A_\mathrm{m}(\lambda)$ as

$$\Delta A_\mathrm{m}(\lambda) = \sqrt{\frac{\sum_{i=0}^{3} \left[ A_{E(i+1)D(0)}(\lambda) - A_{E(i)D(0)}(\lambda) \right]^2}{4}}. \quad (13)$$

In the same manner, $\Delta A_\mathrm{b}(\lambda)$ was defined as

$$\Delta A_\mathrm{b}(\lambda) = \sqrt{\frac{\sum_{i=0}^{3} \left[ A_{E(0)D(j+1)}(\lambda) - A_{E(0)D(j)}(\lambda) \right]^2}{4}}. \quad (14)$$

$\Delta A_\mathrm{m}(\lambda)$ and $\Delta A_\mathrm{b}(\lambda)$ are shown in figure 4(a) and (b), respectively. The absorbance spectra of melanin and blood dissolved in saline are shown in figures 4(a) and (b), respectively.

The shapes of the absorbance spectra are equivalent to $\varepsilon_\mathrm{m}(\lambda)$ and $\varepsilon_\mathrm{b}(\lambda)$ if the scattering effects are ignored. To compare the absorbance spectra with $\Delta A_i(\lambda)$ $(i = \mathrm{m}, \mathrm{b})$ in figures 4(a) and (b), we find that the shapes and peaks in the latter correspond to those in the former, respectively. The peaks of the absorbance spectra of blood in the shorter wavelength range is much higher than those in the longer wavelength range, while the peaks in the shorter wavelength range $\Delta A_\mathrm{b}(\lambda)$ are lower than those in the longer wavelength range. This is because $\bar{l}_i(\lambda)$ is shortened by a strong scattering of intralipid and strong absorbance of melanin or blood in the shorter wavelength.

$C_i/\Delta C_i$ $(i = \mathrm{m}, \mathrm{b})$ of all $A_{E(i)D(j)}(\lambda)$ were estimated by multiple regression analysis if $A_0(\lambda)$ and $A_\mathrm{skin}$ in equation (10) were replaced with $A_{E(0)D(0)}(\lambda)$ and $A_{E(i)D(j)}(\lambda)$,
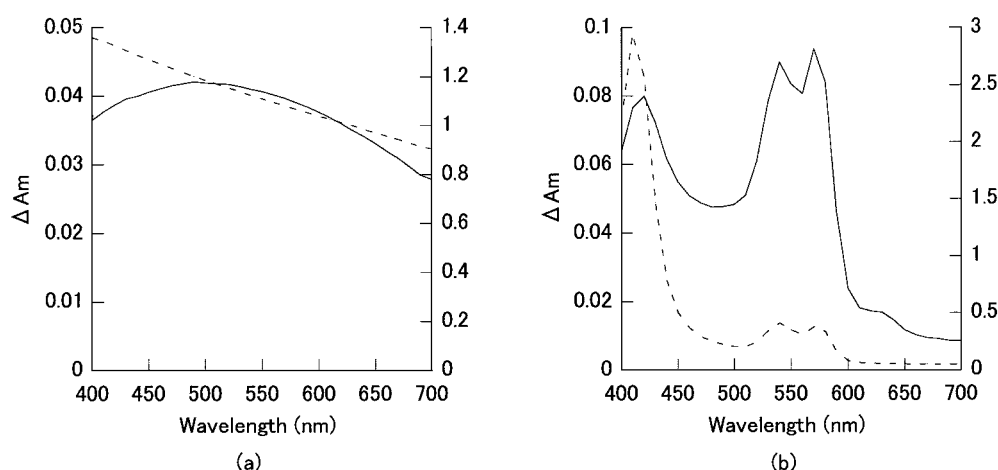
**Figure 4.** (a) Comparison absorption spectrum of melanin solution (full line and left axis) with change in the absorbance spectrum caused by increase in melanin $\Delta A_m(\lambda)$ (dotted line and right axis). $\Delta A_m(\lambda)$ includes the effect of scattering of skin phantom. (b) Comparison of the absorption spectrum of the blood solution (full line and left axis) with change in absorbance spectrum caused by increase in blood $\Delta A_b(\lambda)$ (dotted line and right axis). $\Delta A_b(\lambda)$ includes effect of scattering of skin phantom.
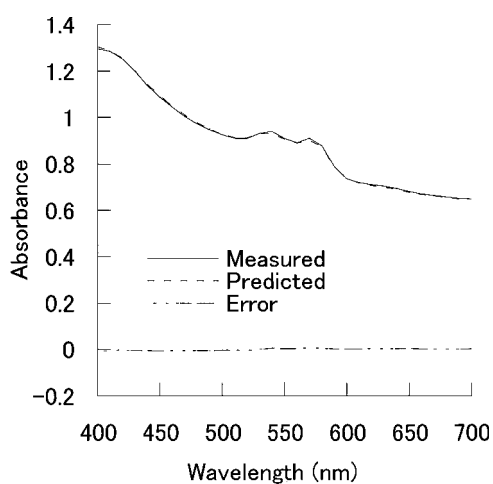


**Figure 5.** Typical estimated absorbance spectrum of $E(3)D(2)$ skin phantom by the multiple regression analysis in which predictor variables are $\Delta A_m(\lambda)$ and $\Delta A_b(\lambda)$. $R^2$ of $\hat{A}_{E(3)D(2)}(\lambda)$ is 0.998.

respectively. The typical estimated absorbance spectrum is shown in figure 5. $R^2$ averaged over 25 three-layered skin phantoms is 0.977. This result shows that estimation by multiple regression analysis is reasonable.

We defined weight concentration $C'$ as $C/M$ where $M$ is a molecule of absorption material. The comparison $C'_i$ ($i$ = m, b) with $\hat{C}'_i$ ($i$ = m, b) which is estimated as $C'_i$ ($i$ = m, b) is shown in figure 6. The coefficient of correlation for melanin and blood are 0.996 and 0.948, respectively. The errors of estimated concentration were defined as $|C'_m - \hat{C}'_m|/C'_m$ and $|C'_b - \hat{C}'_b|/C'_b$ except that the concentrations are zero. The averaged error for blood is 0.17 while the averaged error for melanin is 0.097. The high error for blood is caused by change in $\bar{l}_b(\lambda)$.
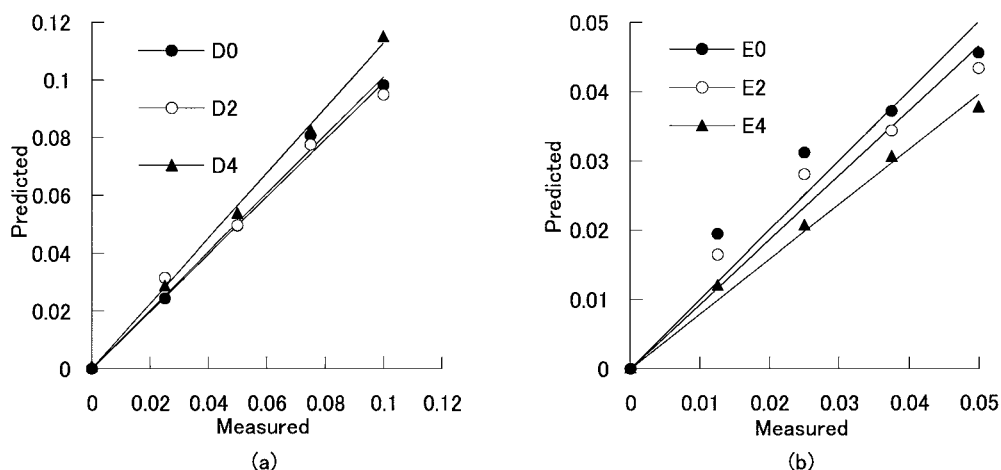
**Figure 6.** (a) Estimated melanin concentration of $E(i)D(0)$, $E(i)D(2)$, $E(i)D(4)$ ($i = 0, 1, 2, 3, 4$). (b) Estimated blood concentration of $E(0)D(j)$, $E(2)D(j)$, $E(4)D(j)$ ($j = 0, 1, 2, 3, 4$).
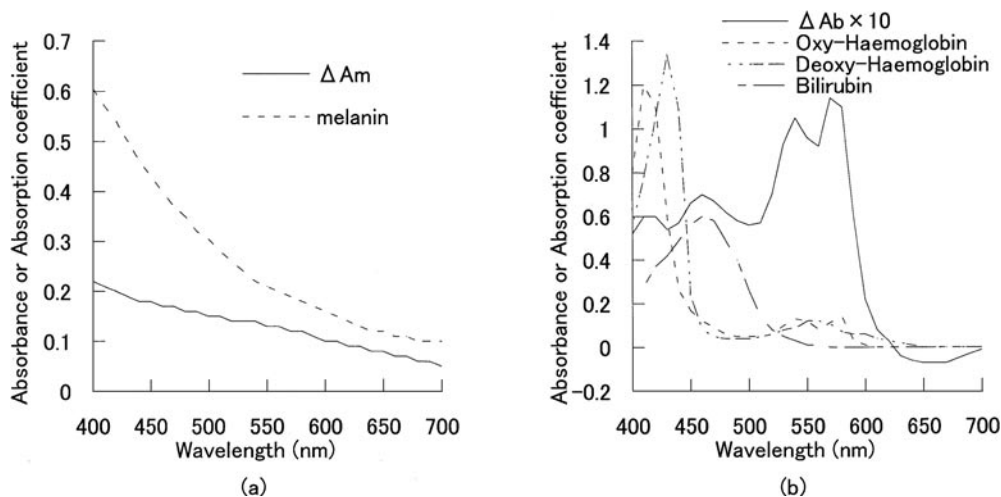


**Figure 7.** (a) Comparison of the molar absorption spectra of melanin $\varepsilon_{\mathrm{m}}(\lambda)$ with change in absorbance spectrum between before and after 16 days $\Delta A_{\mathrm{m}}(\lambda)$. Slope of $\Delta A_{\mathrm{m}}(\lambda)$ is gentler than $\varepsilon_{\mathrm{m}}(\lambda)$ because the scattering of human skin in shorter wavelength is stronger than that in longer wavelength. (b) Comparison of the molar absorption spectra of oxy-haemoglobin, deoxy-haemoglobin and bilirubin with change in absorbance spectrum between before and after 2 min $\Delta A_{\mathrm{b}}(\lambda)$. Sizes of peaks of $\Delta A_{\mathrm{b}}(\lambda)$ are different from those of oxy-haemoglobin and bilirubin while wavelength of the peaks correspond.

## 5. Estimation of melanin and blood concentration in the human skin *in vivo*

The concentration of melanin maximizes about 2 weeks after exposed by UV ray. By subtracting the absorbance spectrum after 16 days from that before, we can obtain the change in this spectrum which is assumed to be caused by melanin increase in the skin. As the same skin phantom, $\Delta A_{\mathrm{m}}(\lambda)$ was defined as a square root of the average of the square of change in the absorbance spectra over the three persons. Figure 7(a) describes $\Delta A_{\mathrm{m}}(\lambda)$ and the molar
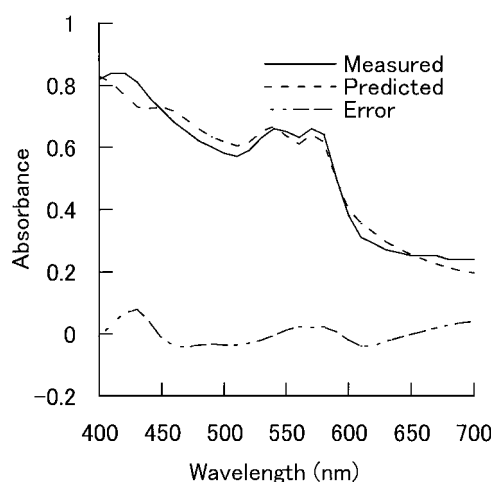
**Figure 8.** Typical estimated absorbance spectrum of human skin *in vivo* by multiple regression analysis in which predictor variables are $\Delta A_m(\lambda)$ and $\Delta A_b(\lambda)$. $R^2$ is 0.973.

absorption spectrum of melanin (Anderson *et al* 1980, Anderson and Parrish 1981). The shape of $\Delta A_m(\lambda)$ is monotonic to the wavelength and similar to the molar absorption spectrum of melanin. $\Delta A_m(\lambda)$, however, is distorted by the scattering effect and the slope is gentler than in the molar absorption spectrum.

The change in the absorbance spectra before and after bathing is supposedly caused by an increase in blood in human skin. $\Delta A_b(\lambda)$ was defined in the same manner from the change in the absorbance spectra before and after 2 min of the five persons. Figure 7(b) shows $\Delta A_b(\lambda)$ and the molar absorption of three chromophores in blood: oxy-haemoglobin, deoxy-haemoglobin and bilirubin. Comparing the molar absorption spectra of the three chromophores with $\Delta A_b(\lambda)$, we find $\Delta A_b(\lambda)$ were distorted by $\bar{l}_i(\lambda)$. The distortion for blood is larger than for melanin because the scattering and thickness of dermis are larger than in the epidermis.

Equation (10) was applied to the absorbance spectra of *in vivo* skin to perform multiple regression analysis. $A_0(\lambda)$ for *in vivo* skin was supposed to be independent of wavelength. The typical estimated absorbance spectrum is in good agreement with the measured one in figure 8. The average of $R^2$ is 0.975 for eight persons.

Figure 9(a) shows estimated $C_m/\Delta C_m$ and estimated $C_b/\Delta C_b$ which were obtained from the absorbance spectra of skin exposed to UV light. After exposure to UV light, blood in human skin increased temporarily and then returned to normal condition, while melanin increased monotonously. Figure 9(a) clearly describes these phenomena. In the same manner, figure 9(b) shows estimated $C_m/\Delta C_m$ and estimated $C_b/\Delta C_b$ which were obtained from the absorbance spectra of skin bathing in hot water. After bathing in hot water, blood in human skin increases while melanin does not change. Figure 9(b) clearly describes these phenomena too.

## 6. Conclusion and discussion

The absorbance spectra of human skin and skin phantoms were clearly explained by $\Delta A_m(\lambda)$ and $\Delta A_b(\lambda)$ caused by a change in melanin and blood concentration using multiple regression analysis based on the modified Beer–Lambert law. If $\Delta C_m$ and $\Delta C_m$ are known, it is possible to estimate melanin and blood concentration in a short calculation time.
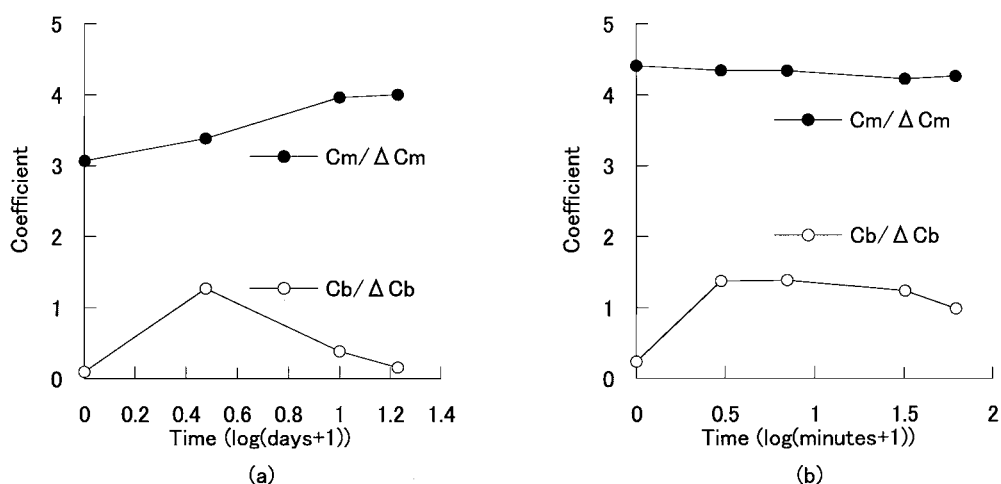
**Figure 9.** Measured and estimated concentration of a typical human skin exposure (a) to UV light and after (b) bathing in hot water. Time transition of concentration of melanin and blood correspond to the medical viewpoint.

If the change in concentration of chromophores is large, $\Delta A_i(\lambda)$ is not proportional to $\Delta C_i$ (Delpy *et al* 1988, Matcher *et al* 1993) because $\bar{l}_i(\lambda)$ decreases as the concentration of chromophores increases. What is worse, the absorbance of the whole blood is a non-linear function of the concentration of haemoglobin (Lipowsky *et al* 1980). The non-linear effect should be considered for high accuracy measurement.

We should pay attention to the change of oxygen in blood after burns. $\Delta A_b(\lambda)$ at 600–700 nm is negative because of an increase in oxy-haemoglobin whose molar absorption coefficients are smaller than deoxy-haemoglobin. The individual variations of $\Delta A_b(\lambda)$ are so large that some spectra do not have a peak of bilirubin, the other spectra have the largest peak at 430 nm.

The increase of absorbance spectra caused by increase in melanin and the strong scattering of human skin are large at the shorter wavelength and gradually decrease as the wavelength is longer. It is difficult to distinguish these effects. Estimated $C_m$ causing lack of melanin is not zero.

The $R^2$ of all spectra of human skin is higher than 0.95. Our model is not complete but reasonable for expressing the macroscopic light propagation of human skin.

## Acknowledgments

## References

Anderson R R, Hu J and Parrish J A 1980 Optical radiation transfer in the human skin and applications in *in vivo* remittance spectroscopy *Bioengineering and Skin* ed R Marks and A P Payne (London: MTP Press) pp 253–65
Anderson R R and Parrish J A 1981 The optics of human skin *J. Invest. Dermatol.* **77** 13–9
Barton J K, Pfefer T J and Welch A J 1998 Optical Monte Carlo modeling of a true port wine stain anatomy *Opt. Exp.* **2** 391–6
Delpy D T, Cope M, van der Zee P, Arridge S, Wray S and Wyatt J 1988 Estimation of optical path length through tissue from direct time of flight measurement *Phys. Med. Biol.* **33** 1433–42

Feather J W, Ellis D J and Leslie G 1988 A portable reflectometer for the rapid quantification of cutaneous heamoglobin and melanin *Phys. Med. Biol.* **33** 711–22

Hasegawa Y, Yamada Y, Tamura M and Nomura Y 1981 Monte Carlo simulation of light transmission through living tissues *Appl. Opt.* **30** 4515–20

Hiraoka M, Firbank M, Essenpreis M, Cope M, Arridge S R, van der Zee P and Delpy D T 1993 A Monte Carlo investigation of optical path length in inhomogeneous tissue and its application to near-infrared spectroscopy *Phys. Med. Biol.* **38** 1859–76

Imai F H, Tsumura N, Haneishi H and Miyake Y 1996 Principal component analysis of skin color and its application to colorimetric color reproduction on CRT display and hardcopy *J. Imaging Sci. Technol.* **40** 422–30

Johnson R A and Bhattacharyya G K 1996 *Statistics Principles and Methods* 3rd edn (New York: Wiley) ch 11 and 12

Kienle A, Lilge L, Vitkin I A, Patterson M S, Wilson B C, Hibst R and Steiner R 1996 Why do veins appear blue? A new look at an old question *Appl. Opt.* **35** 1151–60

Lipowsky H H, Usami S and Chien S 1980 Hematocrit determination in small bore tubes from optical density measurements under white light illumination *Microvasc. Res.* **20** 51–70

Lu J Q, Hu X H and Dong K 2000 Modeling of the rough-interface effect on a converging light beam propagating in a skin tissue phantom *Appl. Opt.* **39** 5890–7

Matcher S J, Cope M and Delpy D T 1993 Use of the water absorption spectrum to quantify tissue chromophore concentration changes in near-infrared spectroscopy *Phys. Med. Biol.* **38** 177–96

Nomura Y, Hazeki O and Tamura M 1997 Relationship between time-resolved and non-time-resolved Beer–Lambert law in turbid media *Phys. Med. Biol.* **42** 1009–22

——1989 Exponential attenuation of light along nonlinear path through the biological model *Adv. Exp. Med. Biol.* **248** 77–80

Shimada M, Masuda Y, Yamada Y, Itoh M, Takahashi M and Yatagai T 2000 Explanation of the human skin color by multiple linear regression analysis based on the modified Lambert–Beer law *Opt. Rev.* **7** 348–52

Tsumura N, Sato H, Hasegawa T, Haneishi H and Miyake Y 1999a Limitation of color samples for spectral estimation from sensor responses in fine art painting *Opt. Rev.* **6** 57–61

Tsumura N, Haneishi H and Miyake Y 1999b Independent-component analysis of skin color image *J. Opt. Soc. Am.* A **16** 2169–76

van Gemert M J C, Jacques S L, Sterenborg H J C M and Star W M 1989 Skin Optics *IEEE Trans. Biomed. Eng.* **36** 1146–54

Verkruysse W, Lucassen G W and van Gemert M J C 1999 Simulation of color of port wine stain skin and its dependence on skin variables *Lasers in Surgery and Medicine* **25** 131–9

Wan S, Anderson R R and Parrish J A 1981 Analytical Modeling for the Optical Properties of the Skin with *in vitro* and *in vivo* Applications *Photochem. Photobiol.* **34** 493–9

Wang L and Jacques S L 1992 Monte Carlo modeling of light transport in multi-layered tissues in Standard C M D Anderson Cancer Center/Texas University, Texas

Wang L, Jacques S L and Zheng L 1995 MCML-Monte Carlo modeling of light transport in multi-layered tissues *Computer Methods and Programs in Biomedicine* **47** 131–46